Supplementary Information (SI) for Journal of Materials Chemistry A.
This journal is © The Royal Society of Chemistry 2025

Low temperature and fast response TEA sensor based on n-n WO3/In2O3 heterojunctions

Shuwen Zhu [a], Huiqing Fan [a, *], Yuxin Jia [a], Yongbo Fan [b], Weijia Wang [a, *]

[a] *State Key Laboratory of Solidification Processing, School of Materials Science and Engineering, Northwestern Polytechnic University, Xi'an 710072, China*

[b] *School of Electronics and Information, Northwestern Polytechnical University, Xi'an 710072, P. R. China*

[c] *Department of Applied Physics, The Hong Kong Polytechnic University, Hung Hom 100872, Hong Kong, PR China*

**Corresponding authors.*

E-mail addresses:

hqfan3@163.com, hqfan@nwpu.edu.cn (Prof. H. Q. Fan);

weijia.wang@nwpu.edu.cn (Dr. W. J. Wang);

Experimental details

S1.1 Raw materials and chemical solvent

All the ingredients were directly used without further purification. N, N-Dimethylformamide (DMF), terephthalic acid ($C_8H_6O_4$), soduim acetate anhydrous (NaOAc), triethylamine ($C_6H_{15}N$, TEA), anhydrous ethanol (C_2H_5OH), methanol anhydrous (CH_3OH), formaldehyde solution (HCHO, 37.0%−40.0%), acetone (C_3H_6O), were obtained from Sinopharm Chmical Reagent Co., Ltd. Indium(III) nitrate hydrate ($In(NO_3)_3 \cdot 6H_2O$), Tungsten hexachloride (WCl_6), Glacial acetic acid (HAc) and ammonia solution (H_5NO, 25.0%−28.0%)were purchased from Shanghai Aladdin Biochemical Technology Co., Ltd.

S1.2 Gas sensors fabrication and TEA sensing properties investigation

For maintaining repeatability and improving the electrical contact and mechanical strength, the sensors were thermal aged for 3 days on the thermal aging instrument before measurement. Furthermore, the relative humidity (RH) and ambient temperature were monitored using a moisture and temperature detector inside the test chamber.

The WS-30A instrument (Weisheng Electronics, China) is a typical static gas-sensing instrument. Therefore, the desired concentrations of gases were obtained using the static liquid-gas distribution method. The WS-30A static instrument employed atmospheric air as the reference and dilution gas. During static testing, the exposure of the sensor to the target gas and air can be adjusted by controlling the glass lid of the test chamber (18 L). The gas-sensing measurement of all sensors were conducted under laboratory conditions (35 ± 10% RH, 25 ± 5 °C). The fabricated sensors were connected to the WS-30A instrument by means of a circuit board with 30 test channels. The small Ni- Cr alloy heating wire inside the sensors is employed to heat the sensors to different operating temperatures. When the baseline of resistance in air (R_a) reaches a stable state at a specific operating temperature (environment temperature: 25 ± 5 °C), a defined volume of the target liquid reagent was injected onto a heating groove located within test chamber. Two miniature fans inside the chamber are applied to quickly and homogeneously disperse the liquid vapor. The generated vapor was promptly mixed with air, generating the desired gas detection atmosphere. After sensor resistance in target gas (R_g) changed and reached a new equilibrium state, the glass cover was removed for the quick gas desorption and maintained until the sensor recovered to its initial value. A few minutes later, the chamber was sealed and the above process was repeated. Each test was carried out three times in parallel under the same conditions and finally averaged.

The TEA and interfering gas (C_2H_5OH, CH_3OH, NH_3, HCHO, C_3H_6O) can be obtained by evaporating the corresponding analytic reagent solution on a heating groove, which is located in the chamber of the WS-30A measuring equipment. The injected volume can be calculated using the **equation.S1**:

$$V_x = \frac{C \times M \times V}{22.4 \times D \times \rho \times 10^{-9}} \tag{S1}$$

Where V_x is liquid injection volume (ml), V is the test box volume (ml), C is the liquid vapor density (ppm), M is the liquid molecular weight (g), D is the specific gravity of liquid (g/cm^3), ρ is the liquid purity.

The resistances changes were measured to evaluate its sensing performance by the gas response (R: the ratio R_a/R_g, where R_a and R_g were the resistances measured in air and the tested gas atmosphere respectively). Response/recovery time refers to the time required to reach 90 % of the equilibrium value in this experiment.

The actual relative humidity inside the static gas chamber can be controlled by evaporating deionized water (DIW). By injecting a quantitative volume of DIW onto the heating block, the vaporized steam can keep the measured humidity. Two miniature fans inside the chamber were also utilized to homogeneously disperse the liquid vapor and steam during the measurement. The built-in hygrometer of WS-30A and the other hygrometer in the test chamber ensure that the RH value is within a reasonable range (± 3% RH).

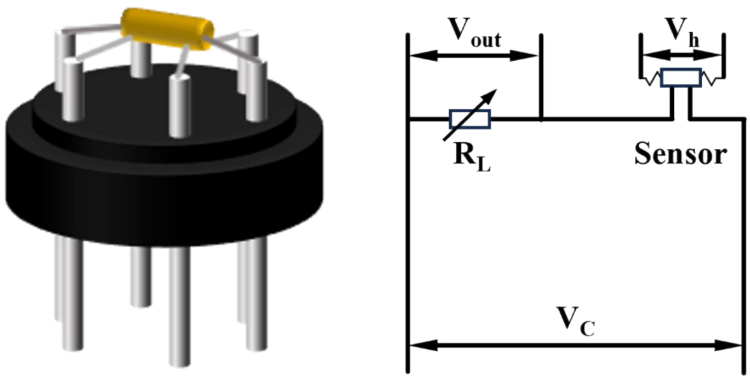

Fig.S1 The sensor device and schematic diagram of gas sensor.

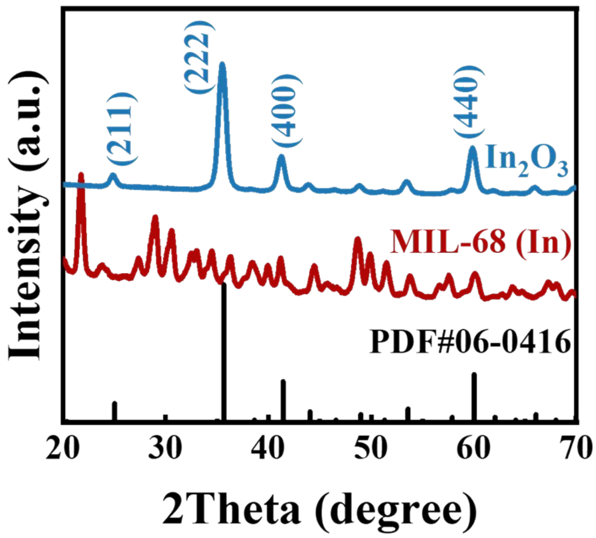

Fig.S2 The XRD pattern of MIL-68(In) and In_2O_3.

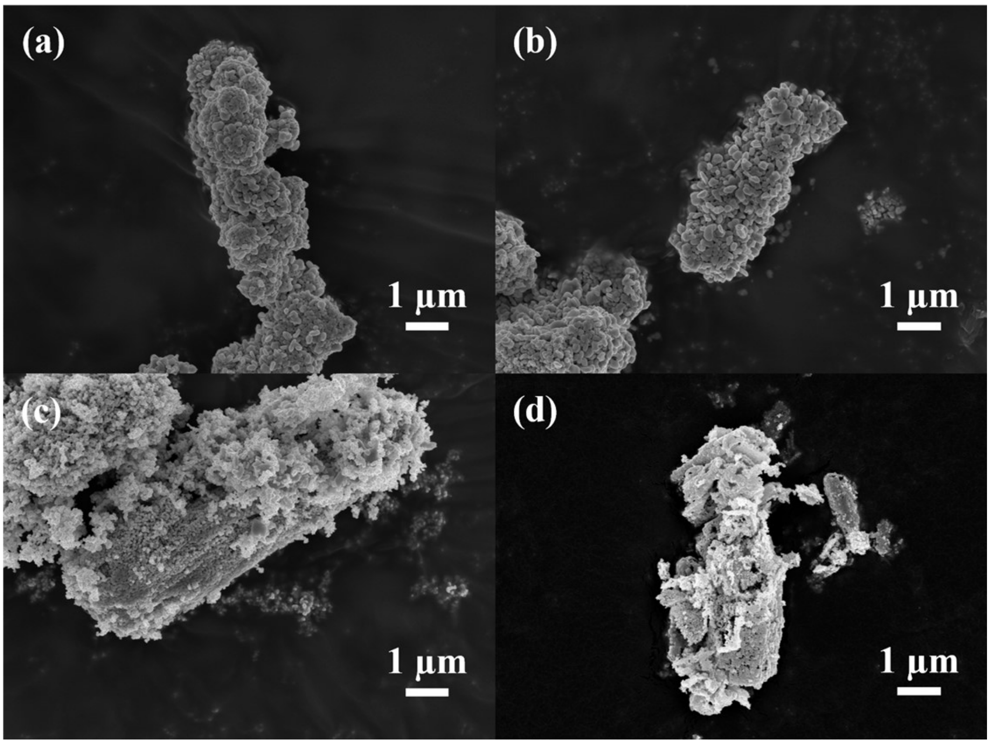

Fig.S3 The SEM images of (a) WO_3/In_2O_3-1, (b) WO_3/In_2O_3-3, (c) WO_3/In_2O_3-4 and (d) WO_3/In_2O_3-5.

Tab.S1 The relative content and ratio of elements W and In obtained from EDS results for WO_3/In_2O_3 heterojunctions.

Materials	W (%)	In (%)	In/W (%, Actual)	In/W (%, theoretical)
WO_3/In_2O_3-1	2.64	0.41	15.53	25
WO_3/In_2O_3-2	1.89	0.43	22.75	50
WO_3/In_2O_3-3	4.36	2.12	48.62	100
WO_3/In_2O_3-4	2.21	3.14	142.08	200
WO_3/In_2O_3-5	2.91	7.68	263.9	400

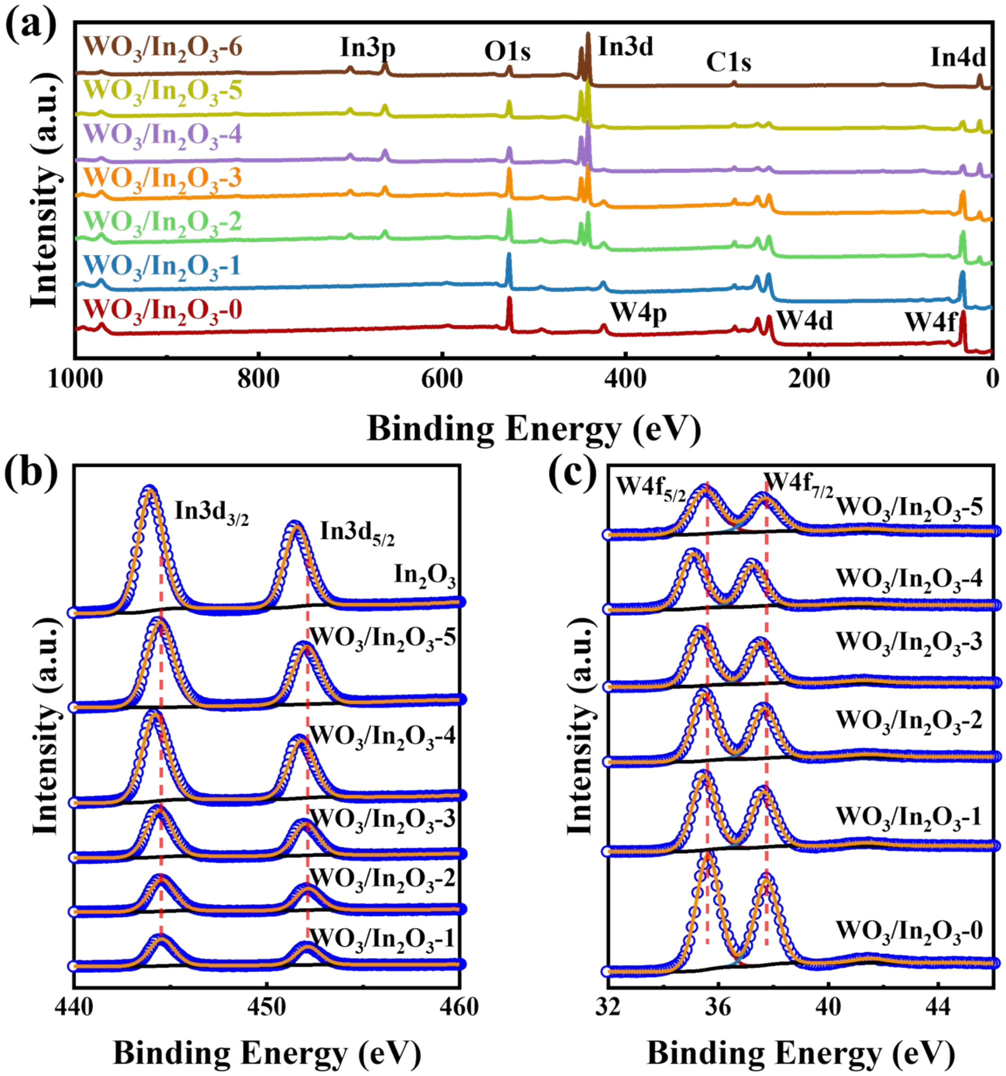

Fig.S4 XPS spectra of (a) full survey spectrum, (b) W4f and (c) In3d for WO_3/In_2O_3 heterojunctions.

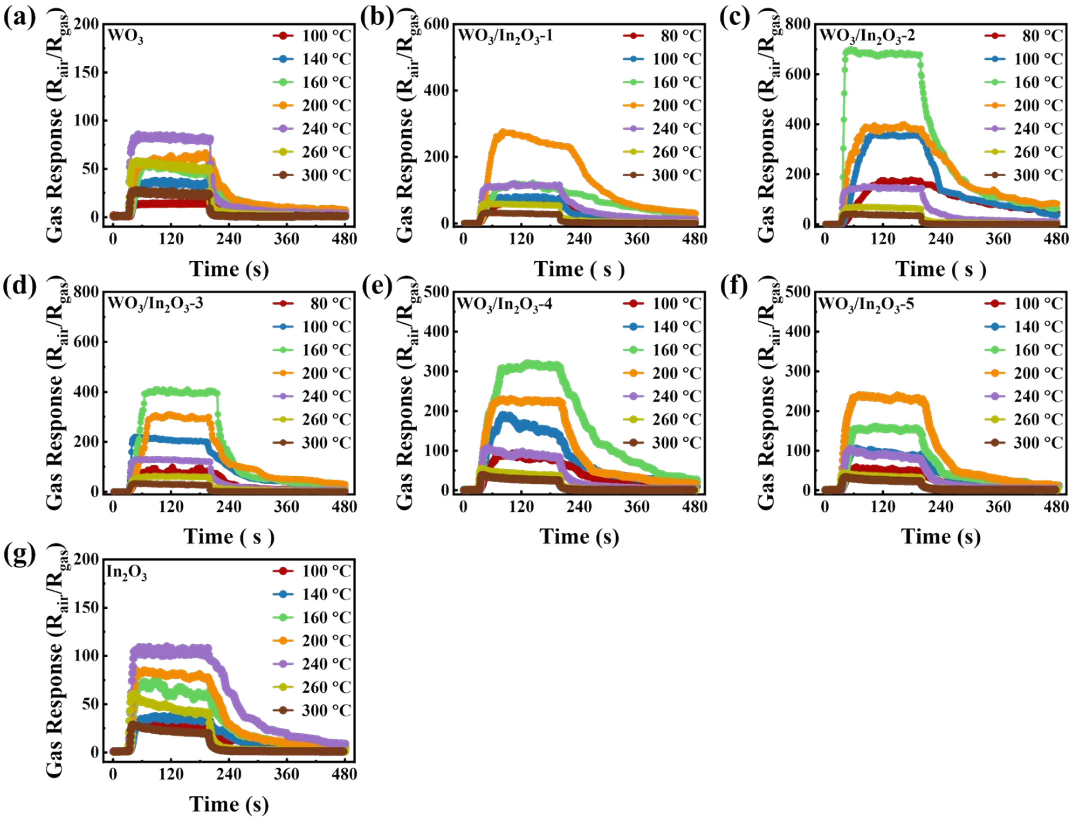

Fig.S5 The gas response transient curves of the WO3, In_2O_3 and WO_3/In_2O_3 heterojunction sensors to 20 ppm TEA at 80-300 °C

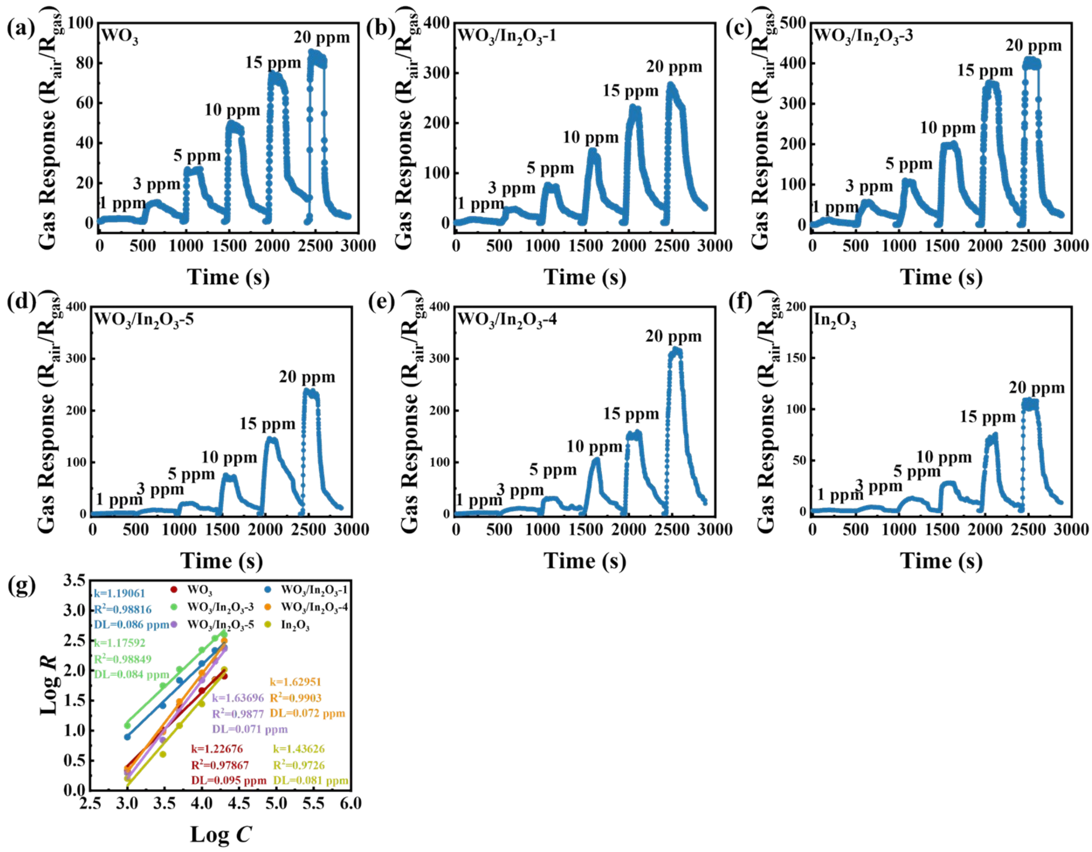

Fig.S6 (a)-(c) The responses of In_2O_3 and WO_3/In_2O_3-0,1,3,4 sensors to 1–20 ppm TEA at optimal operating temperature, (d) the linear relationship of log *S*-log *C* plots to TEA.

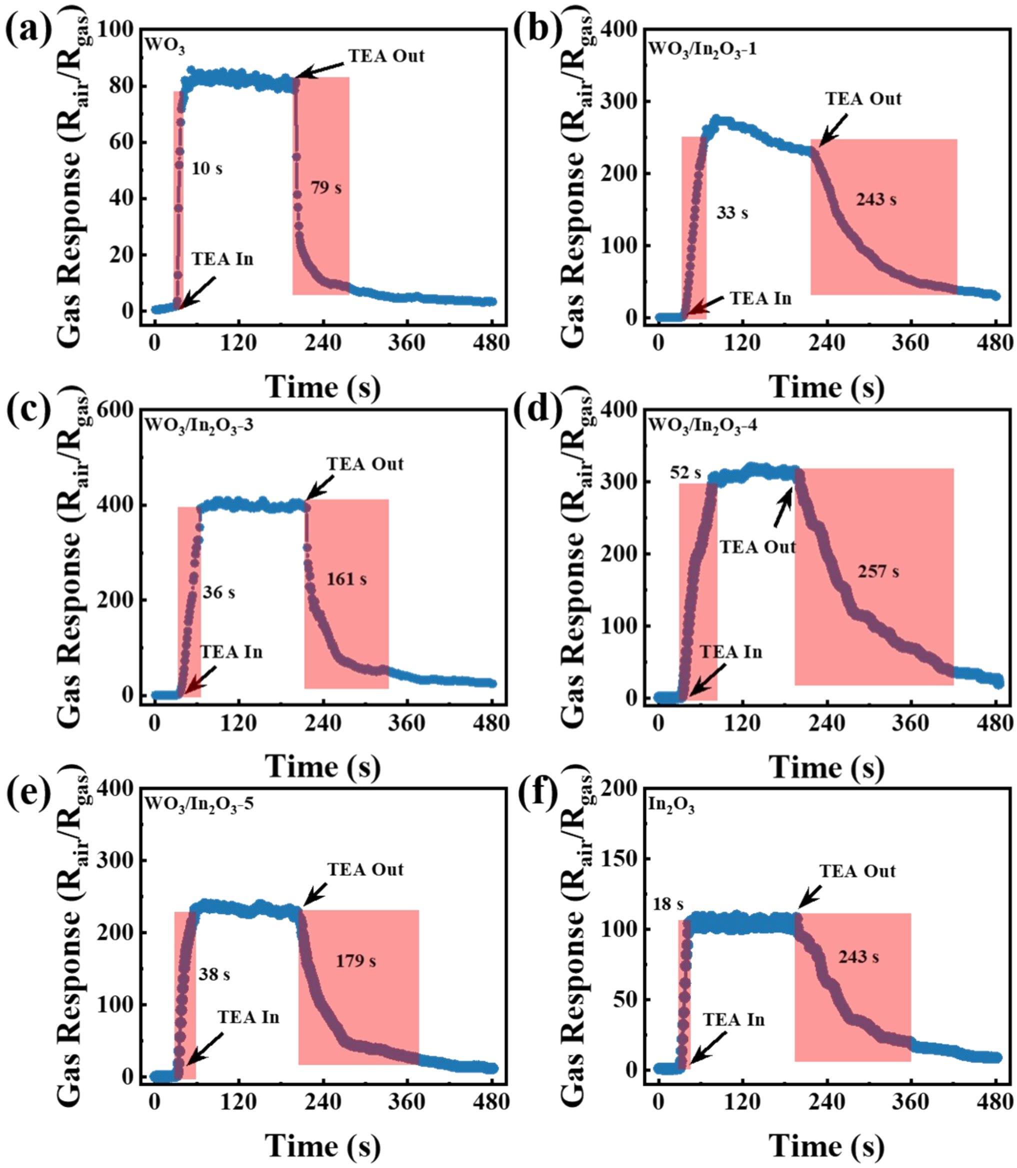

Fig.S7 The response and recovery characteristic curve of In_2O_3 and WO_3/In_2O_3-0,1,3,4 sensors to 20 ppm TEA at optimal operating temperature.

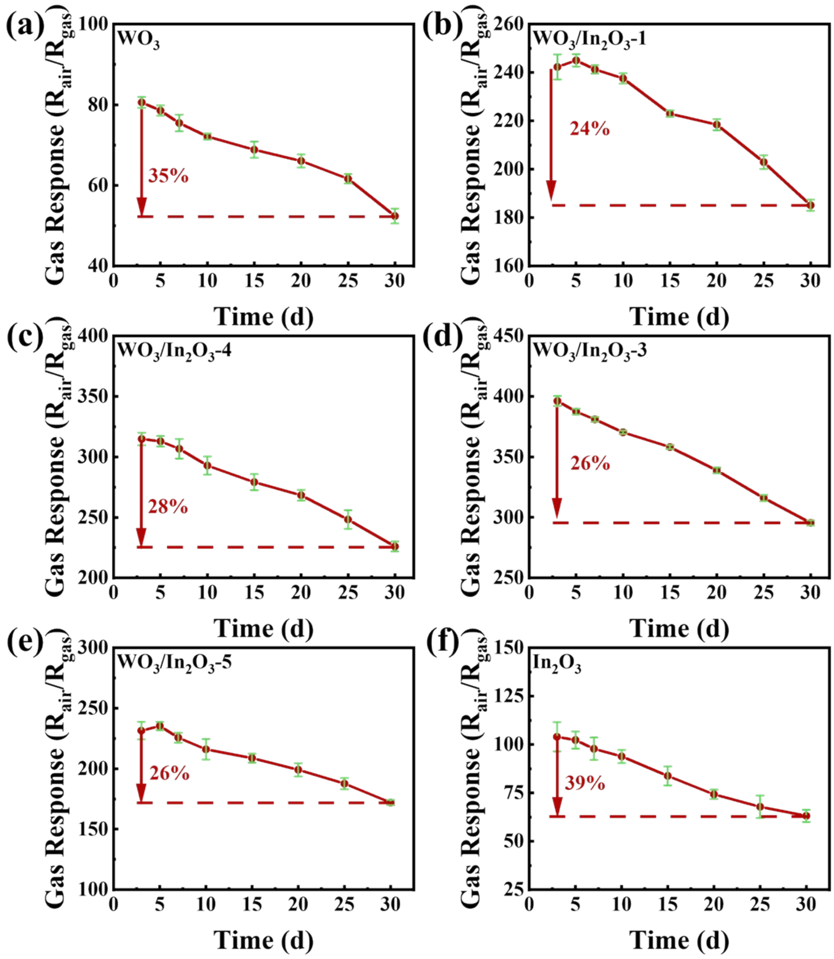

Fig.S8 Long-time stability of resistance of In_2O_3 and WO_3/In_2O_3-0,1,3,4 sensors to 20 ppm TEA at optimal operating temperature for 30 days.

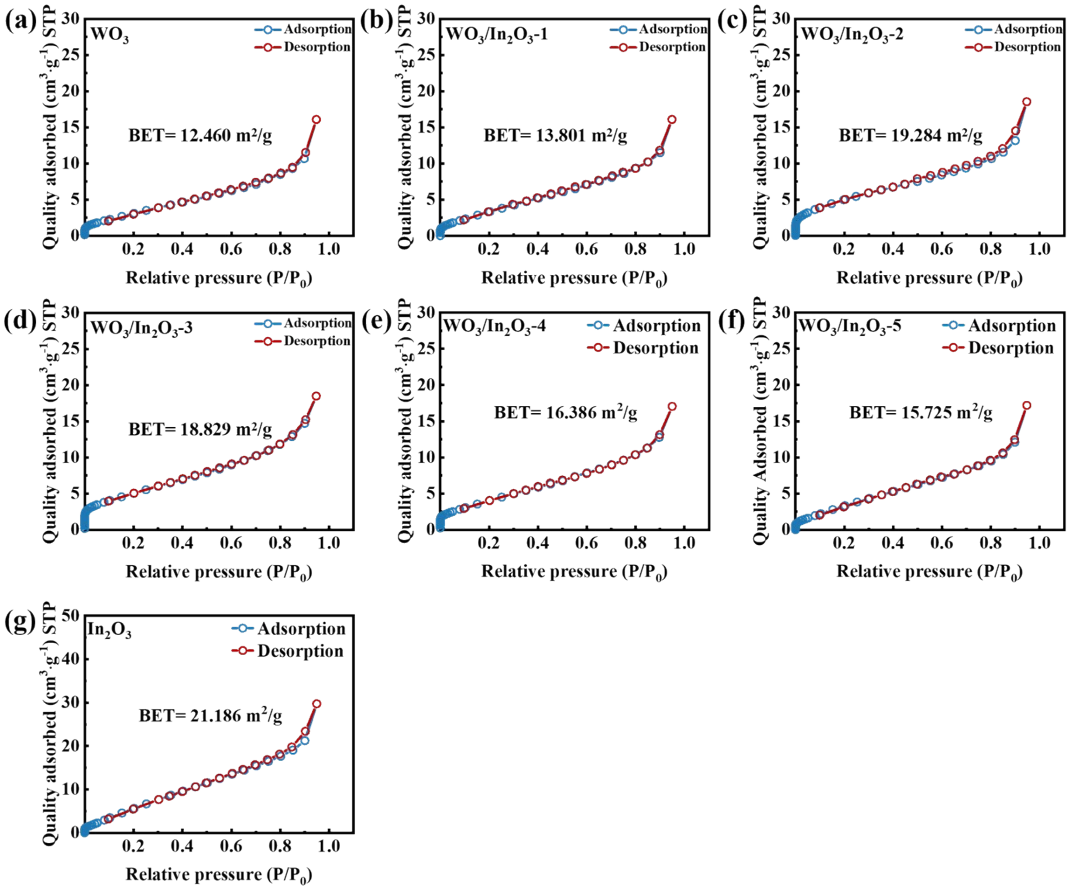

Fig.S9 (a)-(d) The N_2 adsorption/desorption isotherms and BET surface area of WO_3, In_2O_3 and WO_3/In_2O_3 heterojunction.

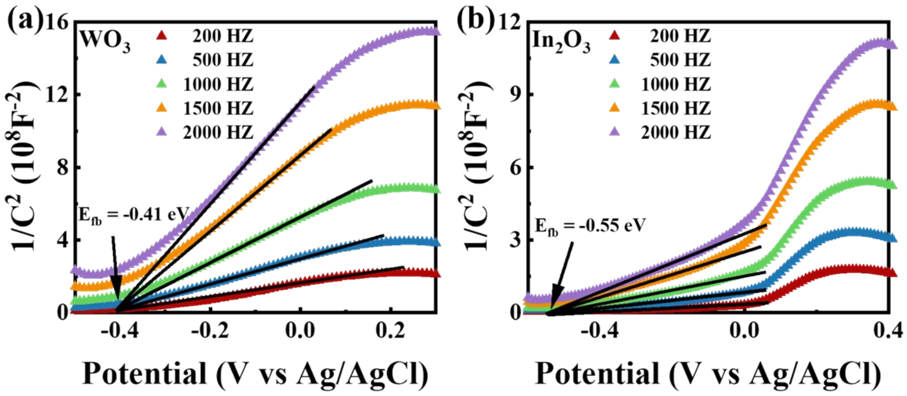

Fig.S10 The Mott–Schottky curves of (a) WO_3 and (b) In_2O_3.

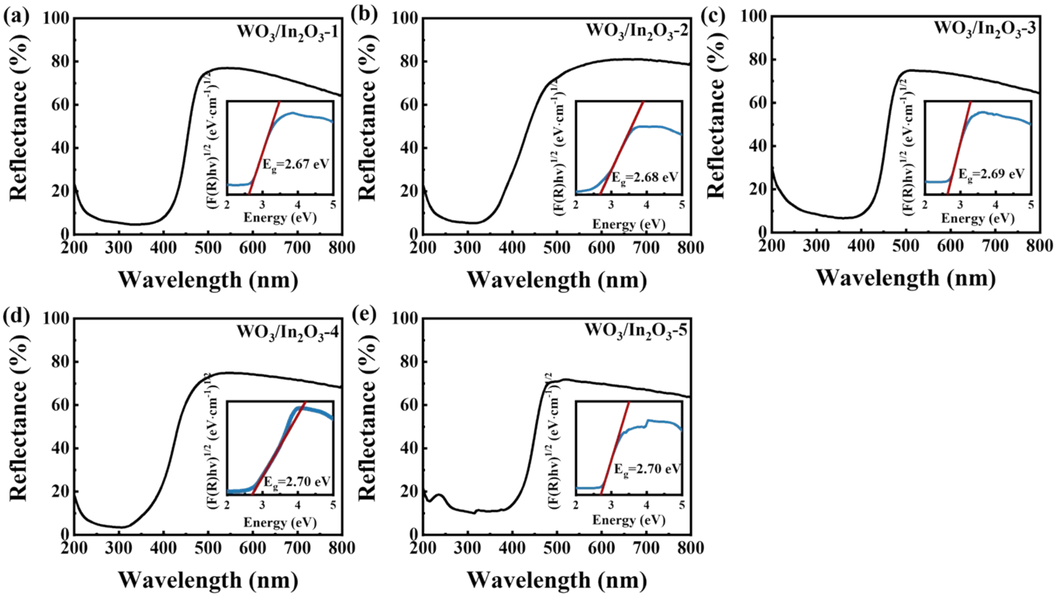

Fig.S11 The UV-vis DRS spectra and plots of transformed Kubelka-Munk function of WO_3/ In_2O_3 heterojunctions.

Tab.S2 Comparison of TEA sensing characteristics of WO_3/In_2O_3 heterojunction sensor with reports of other MOS sensors

Materials	**T (ºC)**	**TEA (ppm)**	**Response**	**τ_{res}/τ_{rec} (s)**	**DL (ppb)**	**Ref.**
$WO_{2.91}$	170	40	6.51	51/-	52	[1]
In_2O_3/ZnO-0.5	200	100	34.87	62/33	1000	[2]
ZrO_2-CeO_2/WO_3	280	20	18.56	1/5	178.9	[3]
WO_3/Fe_2O_3	260	50	30	15/162	1500	[4]
WO_3/In_2O_3	160	20	678.06	11/259	81	This work

Reference:

[1] Z.Q. Zhang, J.X. Liang, K. Liu, W.L. Tian, X. Liang, K. Zhao, et al., Defect-Engineered WO3-x Architectures Coupled with Random Forest Algorithm Enables Real-Time Seafood Quality Assessment, Acs Sensors, 9(2024) 4196-206.

[2] X.Y. Chen, Z. Liu, S. Li, Y. Sun, Y.C. Zhang, Y. Xu, Glycerin-assisted assembly of hierarchical In2O3/ZnO micro-flowers with an in-plane folded shell structure for chemiresistive triethylamine detection, Sensors and Actuators B-Chemical, 418(2024).

[3] W.X. Gao, X.T. Chang, O. Ola, J.A. Han, C.Q. Dai, C. Li, et al., ZrO2-CeO2/WO3 heterostructure films prepared by magnetron sputtering for humidity-tolerant triethylamine sensing, Sensors and Actuators B-Chemical, 418(2024).

[4] Z. Qu, Y. Li, R. Xu, C. Li, H. Wang, H. Wang, et al., Candy-like heterojunction nanocomposite of WO3/Fe2O3-based semiconductor gas sensor for the detection of triethylamine, Microchimica Acta, 190(2023).